Soft Matter

Accepted Manuscript

This is an *Accepted Manuscript*, which has been through the Royal Society of Chemistry peer review process and has been accepted for publication.

Accepted Manuscripts are published online shortly after acceptance, before technical editing, formatting and proof reading. Using this free service, authors can make their results available to the community, in citable form, before we publish the edited article. We will replace this *Accepted Manuscript* with the edited and formatted *Advance Article* as soon as it is available.

You can find more information about *Accepted Manuscripts* in the Information for Authors.

Please note that technical editing may introduce minor changes to the text and/or graphics, which may alter content. The journal's standard Terms & Conditions and the Ethical guidelines still apply. In no event shall the Royal Society of Chemistry be held responsible for any errors or omissions in this *Accepted Manuscript* or any consequences arising from the use of any information it contains.

ROYAL SOCIETY OF CHEMISTRY

www.rsc.org/softmatter

Please do not adjust margins

Journal Name

ARTICLE

Compact Polar Moieties Induce Lipid-Water Systems to Form Discontinuous Reverse Micellar Phase

Received 00th January 20xx,
Accepted 00th January 20xx

DOI: 10.1039/x0xx00000x

www.rsc.org/

Manoj Kumar,[a] Naganath G. Patil,[b] Chandan Kumar Choudhury,[c] Sudip Roy,[c] Ashootosh V. Ambade[b] and Guruswamy Kumaraswamy*[a].

The role of molecular interactions in governing lipid mesophase organization is of fundamental interest and, has technological implications. Here, we describe an unusual pathway for monoolein/water reorganization from a bicontinuous mesophase to a discontinuous reverse micellar assembly, directed by the inclusion of polar macromolecules. This pathway is very different from those reported earlier, where the Fd3m phase formed only upon addition of apolar oils. Experiments and molecular dynamics simulations indicate that hydrophilic ternary additives capable of inducing discontinuous phase formation must (i) interact strongly with the monoolein head group and, (ii) have a compact molecular architecture. We present a detailed investigation that contrasts a monoolein/water system containing polyamidoamine (PAMAM) dendrons with one containing their linear analogs. The Fd3m phase forms only on addition of PAMAM dendrons but not their linear analogs. Thus, the dendritic architecture of PAMAM plays an important role in determining lipid mesophase behavior: Both dendrons and their linear analogs interact strongly with monoolein, through their amine groups. However, while linear polymers adsorb and spread on monoolein, dendrons form aggregates that interact with the lipid. Dendrons induce formation of an intermediate reverse hexagonal phase, which subsequently restructures into the Fd3m phase. Finally, we demonstrate that other additives with compact structures and that are known to interact with monoolein, such as branched polyethylenimine and polyhedral silsesquioxane cages, also induce formation of the Fd3m phase.

Introduction

Nature abhors voids. Ordered assemblies of oil-in-water micelles form readily since water occupies the interstitial spaces in such assemblies.[1,2] Formation of reverse (water-in-oil) micellar assemblies is, however, inhibited by packing frustration. Consider, for example, a reverse hexagonal (H_{II}) phase. Here, micellar cylinders are organized in a hexagonal lattice with a packing fraction of 91%. The 9% "void" space is filled, either by stretching hydrophobic lipid tails or by distorting the micellar cylinders towards a hexagonal cross-section.[1,3] Even more significant packing constraints are encountered by reverse micellar cubic assemblies. Curiously, the Fd3m phase[4] with a packing fraction of 71%, forms more readily than fcc or hcp phases (with higher packing fractions of 74%). The Fd3m phase is comprised of micelles of two distinct sizes organized in a cubic AB_2 lattice (Fig. 1). It has been suggested that preferential formation of the Fd3m phase relative to more densely packed cubic phases may be attributed to lower free energy cost for stretching lipid tails.[5] Fd3m phases have been reported[6,7] for lipid/water systems where the lipids have hydrocarbon tails that are long or branched. Packing frustration in the Fd3m phase can also be reduced by solvating lipid tails through addition of an apolar ternary component. Thus, for hydrophobic lipids such as monolinolein, phytantriol or monoolein, Fd3m phases form on adding hexadecane or tetradecane oil,[8-10] limonene[11] or vitamin E acetate.[12] Recently, the influence of apolar ternary additives on membrane curvature has been analysed in detail[13,14] by accounting for the effect of the additive on membrane rigidity and on lipid tail solvation. Here, we report that a new pathway to the Fd3m phase can be opened, by addition of small quantities of polar, water soluble moieties to a monoolein/water system. We demonstrate that perfectly branched polyamidoamine (PAMAM) dendrons, branched polyethylenimine and silsesquioxane cages induce formation of the Fd3m reverse micellar phase in a monoolein/water system. Further, we contrast the behavior of PAMAM dendrons with their linear analogs (that do not induce Fd3m phase formation) to demonstrate that compact molecular architecture is critical in the formation of discontinuous phase. Introducing a third component into a lipid/water system can

[a] Complex Fluids and Polymer Engineering, Polymer Science and Engineering Division, CSIR-National Chemical Laboratory, Dr. Homi Bhabha Road, Pune 411008, Maharashtra, India. Phone: +91-20-2590-2182; Fax: +91-20-2590-2618, E-mail: g.kumaraswamy@ncl.res.in
[b] Polymer Science and Engineering Division, CSIR-National Chemical Laboratory, Dr. Homi Bhabha Road, Pune 411008, Maharashtra, India.
[c] Physical Chemistry Division, CSIR-National Chemical Laboratory, Dr. Homi Bhabha Road, Pune 411008, Maharashtra, India.

† Electronic Supplementary Information (ESI) available: Detailed synthetic protocols and NMR, GPC characterization; SAXS, optical microscopy and rheological data; MD simulation details and analysis is presented in ESI. See DOI: 10.1039/x0xx00000x

Soft Matter Accepted Manuscript

Please do not adjust margins

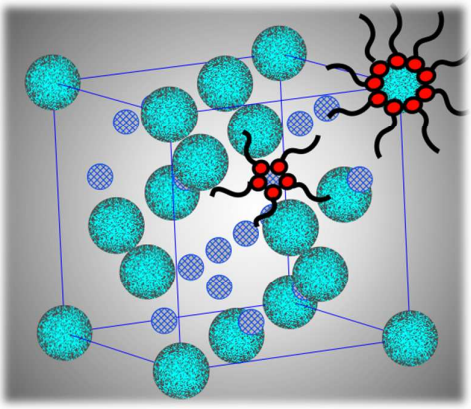

Fig. 1 Schematic of the reverse micellar Fd3m phase with micelles of two different sizes arranged in an AB_2 lattice.

change the mesophase lattice parameter[15-17] or even induce order-order or order-disorder transitions.[18-20] These structural changes significantly affect mesophase properties for example, transition from bicontinuous organization to a discontinuous micellar structure can retard the release of encapsulated molecules by an order of magnitude.[21] Therefore, a fundamental understanding of how ternary inclusions influence lipid/water systems is necessary for rational design of mesophase formulations. This is technologically important since ordered lipid/water mesophases have implications for a wide variety of areas, ranging from control of food texture,[22-24] to biological processes;[25] and from templated syntheses in materials science[26, 27] to protein crystallization[28] and delivery strategies for therapeutic applications.[29-35]

Ternary inclusions can relieve packing frustration, or can affect the local bilayer curvature by changing the effective packing ratio[36] of lipid molecules in the mesophase. In particular, polymeric inclusions strongly affect mesophase organization[37-43] and, offer the added advantage of customization, by copolymerization or by varying molecular weight or chain architecture. Recent simulations[44] indicate that chain architecture of a polymer tethered to a bilayer membrane critically determines its curvature. Inspired by these results, we contrast the effect of poly (amidoamine) (PAMAM) dendrons and their matched linear analogs on the phase behaviour of the technologically important monoolein/water system. PAMAM dendritic structures have attracted attention for their potential in medical applications: PAMAM dendrimers are already in commercial use as high contrast MRI agents.[45] These synthetic constructs afford fractal structures with precise control over the number of functional groups at their periphery and, preserve molecular shape across generations. We begin by describing the phase behaviour of ternary systems containing PAMAM dendrimers in monoolein/water and highlight the role of molecular architecture by contrasting this to monoolein/water containing a linear analog of PAMAM.

MATERIALS AND METHODS:

Glycerol monooleate (called GMO in this work, commercial trade name: Rylo MG 20 Pharma) was received as a generous gift from Danisco Corporation India. Distilled, deionised water, with a resistivity of 18MΩ.cm, was used to prepare the samples. Branched polyethylenimine (bPEI) of $M_w \approx 2000$ g/mol, was obtained from Sigma Aldrich and was used as received. bPEI has a branched architecture and is reported to comprise 25% primary, 50% secondary and 25% tertiary amines. The structure of bPEI was characterized earlier[46] using NMR at different pH. Polysilsesquioxane hydrate-octakis tetramethylammonium substituted (POSS) was obtained from Sigma Aldrich and used as received. Reported procedures were used to synthesize poly-amidoamine (PAMAM) dendrons of various generations (G2, G3 and G4) and their linear analogues (L3, and L4). Detailed procedures are provided in the Supporting Information.

Small angle X-ray scattering (SAXS) experiments were carried out on a Bruker Nanostar machine equipped with a Cu rotating anode, with a tungsten filament (filament size 0.1 x 1mm). The SAXS was operated at a voltage of 45kV and current of 20mA. We used the characteristic Cu K_α radiation (wavelength = 1.54Å), and calibrated the detector with silver behenate. Samples were sandwiched between kapton films and pasted on a metallic holder with a hole for X-rays to pass through. Scattering data was collected on a multiwire gas filled Hi-star 2-D area detector and were reduced to 1-D using the Bruker offline software.

Rheological experiments were performed to determine the mechanical properties of these mesophases. Experiments were carried on the MCR 301 (Anton Paar) using a 8mm parallel plate assembly. Samples were carefully loaded on the plate after allowing several days for equilibration. All tests were carried out at 30°C. Initially, we performed a stress ramp to determine the yield stress for the sample. We then loaded a fresh sample and conducted a creep test at a stress value significantly lower than the yield stress. The viscosity was calculated from the slope of the compliance curve. The yield stress, creep test parameters and viscosity are shown in Supporting Information (Table ST1).

We performed optical microscopy between crossed polarizers on GMO/water/additive systems, to visualise their textures and identify phases. We used a Nikon Eclipse E600 POL with a conventional digital camera (Nikon) connected to a PC. Samples were mounted on a Linkam Shear cell CSS450 for controlled heating. The CSS450 stage is equipped with two heaters for the top and bottom plates. The sample was placed on the lower plate and sandwiched with a glass coverslip. The sample was heated at a rate of 5°C/minute up to ~80°C and was subsequently cooled to ambient temperature. We identify the H_{II} phase based on characteristic cone type textures and the L_α phase based on their streak-like textures. Polarized optical microscopy was used to assign the SAXS peaks to the H_{II} and L_α phases, since only a few peaks were observed for these phases. Fd3m and Ia3d phases are isotropic, and exhibit no texture under cross polarisation.

Soft Matter Accepted Manuscript

This journal is © The Royal Society of Chemistry 20xx

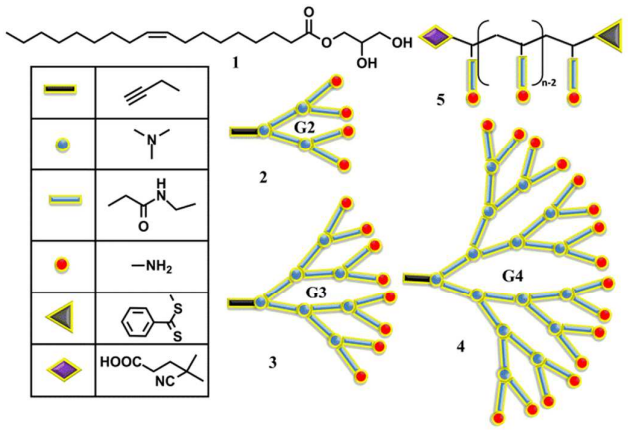

Fig. 2 Schematics of (1) GMO; (2) – (4) G2 to G4 dendrons, respectively and (5) linear analog of the dendrons.

Sample preparation

100 mg of PAMAM dendron (G2, G3, or G4) was added to 100μl of water to prepare a 50 wt% PAMAM/water stock solution. This stock solution was used to prepare GMO/water/PAMAM systems. For example, 500 mg of 80:20:4 GMO/water/G4 was prepared by mixing 384 mg of GMO with 96 mg of water and 40 mg of the PAMAM/water stock solution. This mixture was then heated to ~80°C, and then cooled to room temperature. Samples were stored in a sealed Borosil vial for equilibration. Samples containing other additives or samples at other GMO/water ratios were prepared in a similar manner.

Computational Details:

To obtain detailed insights into the interactions of PAMAM dendrons and their linear analogs with the GMO inverse micellar phase, we performed all atom molecular dynamics (MD) simulations. We employ a three step simulation procedure as described below.

Self-assembly of GMO molecules in water:

The force field for the GMO molecules were adapted from Siu et al.[47] they modified the OPLS-AA force field[48,49] (and termed it L-OPLS) to reproduce the liquid properties (densities, heats of vaporization, and self-diffusions) of long alkanes. They obtained liquid crystalline phase of GMO (at 310 K, above the glass transition temperature, T_g = 290 K) by applying the L-OPLS force field at full hydration (i.e., 1 GMO: 28 Water). Note that the original OPLS-AA force field produces a gel structure for these conditions. The TIP3P-MOD water model was used.[50] We have constructed the same system of GMO-water as Siu et al. by placing 256 GMO lipid molecules and 28 water molecules per lipid, randomly in the simulation box. This simulation box was further subjected to MD simulation at 310 K, which resulted into self-assembled bilayer structure. This self-assembled structure was replicated twice in the bilayer direction to form a larger system with 512 lipid molecules and was simulated for 100 ns [see SI Fig. S21 for final snapshot]. Henceforth, this system is referred as GMO-water system. The area per lipid was 0.336 ± 0.004 nm^2, close to the experimental area[51,52] per lipid of 0.34 nm^2 or 0.36 nm^2 at 310 K.

Polymer in water:

9 G4 PAMAM (G4) and 12 L-PAMAM were simulated in water for 10 ns before incorporating them in the bilayer-water system. OPLS-AA force field for amines[53] and amides[49] were used for G4[54-55] and TIP3P-MOD[50] was used as the water model. The force field parameters for G4 employed in this study are presented in Table ST4-ST6. The average radius of gyration, R_g, for the single chain of G4 in water was 1.10 nm, which is in agreement with experimental value of 1.24 nm[56] this, validates the force field for G4. L-PAMAM was slightly modified from the experimental L4 molecule to avoid the non-trivial procedure of parameterization and validation of the force fields [see SI Fig. S20a]. We replaced the terminal benzodithioate acid group with a phenyl moiety and the other terminal cynomethylbutanoic acid group with a methyl. This modification of L-PAMAM did not lose the significance of amine functional groups that are present in the repeating units. Since the modified L-PAMAM had similar functional groups as G4, we have used same OPLS-AA atom types as G4. The force field parameters are presented in SI Table ST4-ST6. This is justified as the OPLS-AA force field had been applied and validated by reproduction of experimental thermodynamic (density, glass transition temperature, thermal expansion coefficient)[54,55,57-59] and structural (radius of gyration, hydrogen bonds) properties[60] for polyamides and polyamines with different chain length and topologies.

Self-assembled GMO-Water and polymer systems:

To match the 6% concentration of water with that in the experiment, we decreased the water molecules from the self-assembled GMO-water system. On the water phase of this system we inserted the equilibrated 9 G4 and 12 L-PAMAM molecules, separately [refer Fig. 6 for snapshot]. The GMO-G4 and GMO-L-PAMAM contained 3584 water molecules. The GMO-water-G4 and GMO-water-L-PAMAM systems were simulated for 100 and 200 ns, respectively [see Fig. 6 for final snapshots].

For all simulations, periodic boundary conditions were employed in all directions. Bonds involving hydrogen were constrained using the LINCS algorithm,[61] thus an integration time step of 2 fs was used. The neighbor list was updated every 10 steps with the verlet cutoff scheme[56] as implemented in Gromacs 4.6.3.[62] Particle-mesh Ewald (PME) algorithm[63] with grid spacing of 0.12 nm was used for long range electrostatics. The van der Waals potentials were truncated and shifted such that it vanishes at the cut off (1.30 nm), beyond the cut off, a dispersion correction was applied to the energy and pressure.[64] The self-assembly of 256 random GMO molecules were carried out in isothermal-isobaric ensemble at 310 K and 1 Bar using Berendsen thermostat and barostat[65] with time constant of 0.1 ps, compressibility of 4.5e-5 bar^{-1},

Soft Matter Accepted Manuscript

pressure coupling was 0.1 ps. As the experiments were performed at 298 K (above the glass transition temperature), we carried the simulations at 298 K using the v-rescale thermostat algorithm[66] with a time constant of 0.1 ps that was semi-isotropically coupled by Berendsen barostat[65] at 1.0 bar with compressibility 4.5e-5 bar^{-1} in x/y and z dimensions. The time constant for pressure coupling was 0.1 ps. The trajectories were saved after every 10 ps.

Results and discussion

We use reported divergent procedures[67] to synthesize G2, G3 and G4 PAMAM dendrons that display terminal amine groups (Fig. 2; Supporting Information: Synthesis, characterization details; Schemes Sm1, Sm2, SI Fig. S1). A linear analog of G4, that we term L4, with a matched number of amine groups on a methacrylate backbone is prepared using reported procedures[68] (SI: Schemes Sm3, Sm4; SI Fig. S2, S8). We use a commercial sample of monoolein (Rylo MG 20 Pharma, > 95% purity, henceforth referred to as GMO), that has been previously characterized.[35] Monoolein is widely used as a food emulsifier,[69] and more recently has found uses in pharmaceutical applications[70] and as a model lipid for thermodynamic investigations of phase behavior.[71]

An 80/20 (by weight) mixture of GMO/water forms a highly viscous phase, with room temperature creep viscosity on the order of 10^4 Pas (SI: Experimental; Table ST1). With $\Phi = 2\%$ G4 (viz., GMO: water: G4 = 80:20:2), the creep viscosity increases two-fold. For further addition of G4 ($\Phi = 4\%$, 6%), there is nearly a ten-fold increase in viscosity, to above 10^5 Pas (Fig. 3a). In contrast, for systems with $\Phi = 4\%$ L4 (the linear analog of G4) there is a ~3-fold increase in viscosity that, for $\Phi = 6\%$ L4, decreases to a value similar to the neat GMO/water system (Fig. 3a). Thus, the effect of addition of G4 is qualitatively

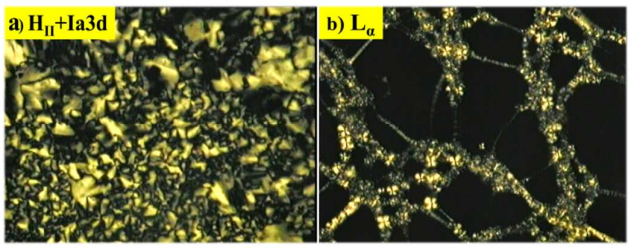

Fig. 4 Optical images for different liquid crystalline mesophases between crossed polarizers. **b)** GMO/water/G4 (85/15/0) streak like features characteristic of the Lα phase are observed; **a)** GMO/water/G4 (80/20/2) fan shaped structures characteristic of the H_{II} phase co-exist with Ia3d phase.

different when compared with L4. We note that experiments repeated at a few selected compositions using high purity (≥99%) monoolein (Aldrich) showed identical results as with GMO (SI Fig. S9), indicating the robustness of our results. The microstructural transformation that underlies this viscosity change is characterized using a combination of small angle X-ray scattering (SAXS) and optical microscopy. Phases are identified using SAXS peak positions: for the Ia3d phase, peaks at q values in the ratio of √6, √8, √14, are observed; at √2, √3, √4, √6, for Pn3m and √3, √8, √11, √12, for Fd3m. Samples are characterized after several days of equilibration at room temperature, when there is no further structural change.

The 80/20 GMO/water system shows a cubic bicontinuous phase with Ia3d symmetry, in accord with previous literature[70] (Fig. 3b). For systems with $\Phi = 2\%$ G4, we observe co-existence of Ia3d and reverse micellar hexagonal (H_{II}) phases (Fig. 3b, H_{II} phase characterized using optical microscopy: Fig. 4a). The discontinuous cubic Fd3m-reverse micellar phase is observed for 4 and 6% G4 (Fig. 3b, SI Fig. S11). For systems with L4, we observe Ia3d and Pn3m co-existence at 4%, and a

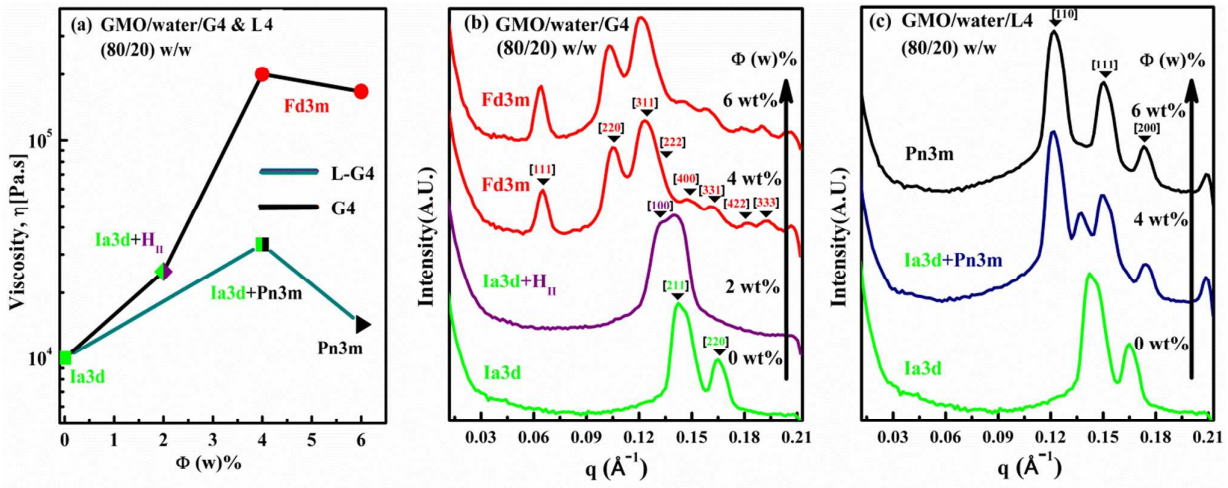

Fig. 3 (a) Creep viscosity of the 80/20 GMO/water system containing the G4 dendron or its linear analog, L4. Φ represents the amount of the ternary inclusion. SAXS data for the 80/20 GMO/water system on addition of (b) G4 and (c) L4.

Soft Matter Accepted Manuscript

This journal is © The Royal Society of Chemistry 20xx

Please do not adjust margins

Journal Name

ARTICLE

transformation into the Pn3m phase at 6% (Fig. 3c). Phase pure bicontinuous cubic phases (with Ia3d and Pn3m symmetry) have comparable high viscosities (~10^4 Pas). Regions of phase coexistence show a 2-3 fold increase in viscosity, while the discontinuous Fd3m micellar phase is associated with significantly higher viscosity, exceeding 10^5 Pas. Formation of an Fd3m phase by addition of hydrophilic molecules to the GMO/water system is unprecedented.

Our results indicate that the chain architecture of the polymeric additive is critical – only the G4 dendron induces formation of the Fd3m phase, while its linear analog (L4) forms the Pn3m phase. Neat 80/20 and 75/25 GMO/water systems form a bicontinuous Ia3d phase while the 85/15 system forms a lamellar (L_α) phase (optical micrograph in Fig. 4b). All three systems form the Fd3m phase at dendron loadings of 6% (Fig. 5, SI Fig. S12–S14).

At higher water concentration, for example 50/50 GMO/water, the cubic Pn3m phase co-exists with excess water. Due to the high viscosity of cubic phases, practical formulations utilize dispersions of Pn3m cubic phase particles in water, termed cubosomes.[73] We note that excess water Pn3m phases with 4% G4 dendrons also transform to discontinuous Fd3m micellar phases (SI Fig. S15). For GMO/water/G4 (Φ = 4%), the Fd3m lattice parameter increases with water content, and saturates at 75/25 GMO/water (SI Fig. S16). For higher water content, the Fd3m phase coexists with excess water. A discontinuous reverse micellar Fd3m phase also forms when second (G2) and third (G3) generation dendrons are added to the 80/20 GMO/water system (Fig. 5; SI Fig. S12–S14). At 2% loading of G2 or G3, there is a transition to an H_{II} phase. At higher dendron concentrations (4% and 6%), we observe a transition to the Fd3m phase (Fig. 5). This progression through the H_{II} phase, to the Fd3m is also observed at GMO/water ratios of 85/15 and 75/25. H_{II} or coexisting H_{II}/Ia3d phases are also observed for GMO/water with 2% G4.

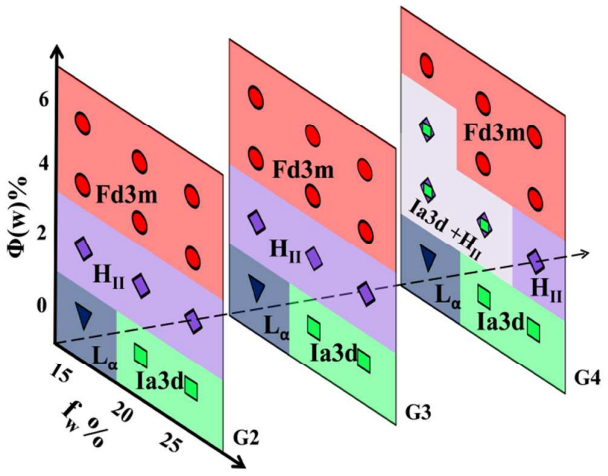

Fig. 5 Equilibrium phase behavior of GMO/water system at room temperature with variation of G2, G3 and G4 dendron content, Φ, and for variation of water content (f_w).

Table 1 Change in lattice parameters obtained from SAXS for the 80/20 GMO/water system with variation of dendron (G2, G3, G4) content, Φ. Different mesophases are obtained at different Φ, as detailed in Figs 3 and 5.

Φ (w)%	G2, a(Å)	G3, a(Å)	G4,a(Å)
0	108	108	108
2	54.2	59.2	--
4	159.3	159.3	162
6	162	166.2	173

Thus, at intermediate dendron concentrations, an H_{II} phase is observed as GMO/water systems transition to the Fd3m phase. In our experiments, samples are heated to high temperatures (≈ 80°C), then cooled to room temperature and allowed to equilibrate over several days. The kinetics of Fd3m phase formation in GMO/water systems containing dendrons is a function of dendron generation. The Fd3m phase forms relatively rapidly for G2 and G3 (~10 days) relative to the G4 (~15 days).

In all cases, an intermediate H_{II} phase forms and is transformed into the Fd3m phase on equilibration (Fig. S15, S17). Hexagonal-cubic phase transitions have been reported[74] in block copolymer systems. In block copolymers, hexagonal cylinders pinch off to form a discontinuous body centered cubic phase. In this context, we note that, for our GMO/water/dendron system, the lattice parameter characterizing the cubic Fd3m phase is always approximately $2\sqrt{2}$ times the H_{II} phase lattice parameter (Table 1; SI Tables ST2, ST3). Thus, our observations suggest that, in analogy to the literature,[75-77] the formation of the Fd3m phase might happen through the breakup of micellar cylinders of the intermediate H_{II} phase. Transition pathways between bicontinuous cubic and H_{II} phases have been previously reported.[75-77] Our results suggest that the discontinuous Fd3m phase forms via an intermediate H_{II} phase, for GMO/water/dendron systems.

Molecular dynamics (MD) studies provide insights into dendron-mediated mechanisms for formation of high curvature inverse micellar phases. We employed MD

Soft Matter Accepted Manuscript

Please do not adjust margins

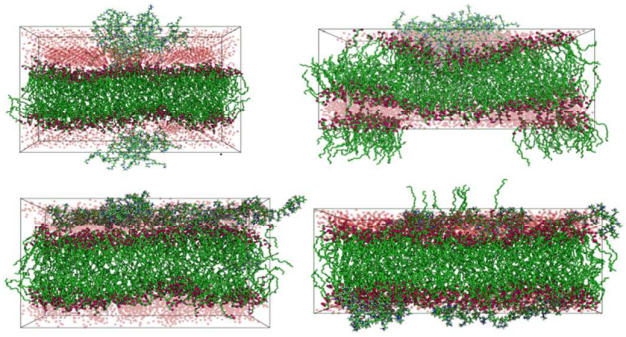

Fig. 6 Snapshots from MD simulations of G4 dendron-GMO/water systems (top) and linear analog-GMO/water systems (bottom). Snapshots on the left represent starting configurations, while right represents structure after 100ns (G4) and 200 ns (linear analog).

simulations (SI Section III) to generate a self-assembled GMO bilayer structure (SI Fig. S21). We introduced 9 G4 molecules (or 12 of their linear analogs, matching the 6% experimental concentration) at the interface of GMO bilayer head groups and water (Fig. 6). Subsequently, we reduced the water content to maintain an 80/20 GMO/water ratio, to match the experiments. We observe aggregation of G4 molecules in water (SI Fig. S22a), driven mainly by intramolecular interactions of *t*-amine moiety with the amido–O (Fig. S23). When this G4 aggregate interacts with the bilayer (Fig. 6), interactions between the dendritic amine and GMO head group result in a peak in the distance distribution function at 0.35 nm (Fig. S23a). This strong amine/GMO interaction drives the bilayer structure to bend, to maximize the number of GMO/amine contacts. The number of contacts between dendritic amine and GMO headgroup oxygen increases with time, as does the bilayer curvature (Fig. S23a).

In contrast (Fig. S24 b), when the linear analog is equilibrated with the GMO bilayer, strong amine-GMO headgroup interactions drive the linear molecule to spread on the bilayer to maximize amine-GMO interactions (Fig. 6, Fig. S24 b). Our simulations suggest that strong attractive interactions between the GMO and amine groups play an important role in determining structure of the lipid assembly. In a control study to verify this, we investigated a ternary system of GMO/water/6% PAMAM G4-PEG, where the terminal primary amines are modified to present an oligomeric ethylene glycol moiety. These systems form only bicontinuous cubic phases and do not exhibit formation of an Fd3m phase (SI Fig. S18), validating the role of GMO/amine interactions indicated by our simulations.

Our simulation results suggest how the structure of water soluble polymeric inclusions induces Fd3m phase formation. Clearly, addition of PAMAM dendrons does not mitigate packing frustration. Rather, strong interactions between the amine groups on the dendrons and the GMO head groups compensate for the increase in free energy due to the increased curvature of the discontinuous micellar phases. Dendrons have a compact molecular architecture. They aggregate to form clusters that interact with the GMO interface and bend it. Linear analogs of the dendrons can access a large number of conformational states. Therefore, these molecules can spread on the GMO surface when they adsorb while, this is not possible for dendrons. While synthesis of perfectly branched dendritic structures is well established, it is significantly easier to access randomly branched molecules, such as, for example, branched polyethylenimine (bPEI) (Fig. S19b).

Branching of macromolecules results in a compact architecture, and, similar to PAMAM, bPEI presents primary amine groups (in addition to secondary and tertiary amines). Addition of Φ = 1% bPEI transforms 80/20 GMO/water from an Ia3d phase to an H_{II} phase. For higher bPEI content, Φ = 2, 4%, we observe the formation of an Fd3m phase (Fig. 7a). Further, we report that other moieties with functional groups that are very different from those present in PAMAM or bPEI, but that have compact molecular structures, and that interact with monoolein, also induce the formation of the Fd3m phase.

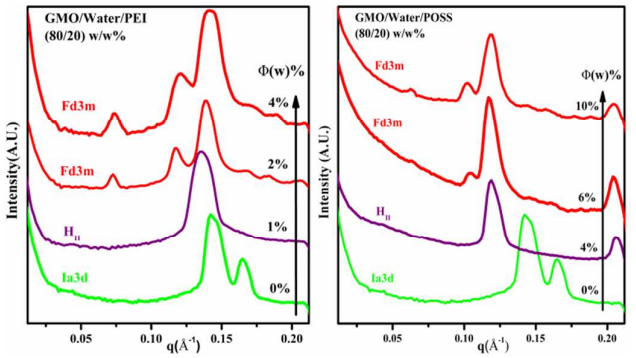

Fig. 7 SAXS data for the a) 80/20 GMO/water containing bPEI ternary additive. Φ represents the amount of bPEI in monoolein/water. b) GMO/water (80/20) containing POSS. Φ represents the amount of POSS in monoolein/water.

It has been reported[56-58,78-80] that negatively charged silica nanoparticles interact with phytantriol, and are effective stabilizers for phytantriol dispersions. As the silica particles used in these reports were several tens of nanometers in size, we used a negatively charged silsequioxane cage as a molecular analog (POSS: Schematic in SI, Fig. S19a). Remarkably, here too, we observed a transformation of an 80/20 monoolein water system from a bicontinuous Ia3d structure to an H_{II} phase (for POSS inclusion at Φ = 2, 4%) and to an Fd3m phase (at Φ = 6, 10%) (Fig. 7b). Our results suggest that addition of compact, interacting polar macromolecular additives to monoolein/water might open a new route to the Fd3m phase, through an intermediate H_{II} phase.

Conclusions

We demonstrate that the monoolein/water system can form a discontinuous reverse micellar Fd3m phase in ternary systems containing polar, water soluble macromolecular additives. Our results demonstrate a new pathway to the Fd3m phase through addition of polar molecules that is very different from previous reports where apolar oils were used as ternary

Soft Matter Accepted Manuscript

This journal is © The Royal Society of Chemistry 20xx

components to access the Fd3m phase. We present selection rules for polar ternary additives that mediate the formation of the discontinuous reverse phase: additives with a compact molecular architecture and that have strong attractive interaction with the monoolein lipid induce formation of the Fd3m phase. We establish the general validity of these criteria by investigating monoolein/water systems containing three very different additives – that are all molecularly compact moieties that interact strongly with monoolein. Monoolein/water systems form Fd3m phases on addition of a few weight percent of PAMAM dendrons, branched PEI and silsesquioxane cages. Remarkably, while PAMAM dendrons induce Fd3m phase formations, their linear analogs with a matched number of amine groups do not. Formation of the Fd3m phase is always preceded by the formation of an intermediate reverse hexagonal phase. This work presents evidence for an unprecedented route to Fd3m phase formation in lipid/water systems. Our work has implications for fundamental understanding of the principles that guide lipid assembly.

Acknowledgements

GK acknowledges funding from the DST Chemical Engineering PAC through project DST/SR/S3/CE/029/2011. AVA acknowledges funding from CSIR (MLP028826). MK acknowledges a research fellowship from UGC. We thank Gaurav Chaudhry from Danisco for supplying us Rylo.

Notes and references

1 G. C. Shearman, A. I. I. Tyler, N. J. Brooks, R. H. Templer, O. Ces, R. V. Law and J. M. Seddon, *Liq. Cryst.,* 2010, **37**(6), 679-694.
2 M. Rappolt, F. Cacho-Nerin, C. Morello and A. Yaghmur, *Soft Matter,* 2013, **9**(27), 6291.
3 G. C. Shearman, A. I. I. Tyler, N. J. Brooks, R. H. Templer, O. Ces, R. V. Law and J. M. Seddon, *J. Am. Chem. Soc.,* 2009, **131**(5), 1678-1679.
4 V. Luzzati, R. Vargas, A. Gulik, P. Mariani, J. M. Seddon and E. Rivas, *Biochemistry,* 1992, **31**(1), 279-285.
5 P. M. Duesing, J. M. Seddon, R. H. Templer and D. A. Mannock, *Langmuir,* 1997, **13**(2), 2655-2664.
6 J. M. Seddon, N. Zeb, R. H. Templer, R. N. McElhaney and D. A. Mannock, *Langmuir,* 1996, **12**(22), 5250-5253.
7 J. M. Seddon, J. Robins, T. Gulik-Krzywicki and H. Delacroix, *Phys. Chem. Chem. Phys.,* 2000, **2**(20), 4485-4493.
8 A. Yaghmur, L. de Campo, L. Sagalowicz, M. E. Leser and O. Glatter, *Langmuir,* 2005, **21**(2), 569-577.
9 A. Yaghmur, L. de Campo, S. Salentinig, L. Sagalowicz, M. E. Leser and O. Glatter, *Langmuir,* 2005, **22**(2), 517-521.
10 A. Chemelli, M. Maurer, R. Geier and O. Glatter, *Langmuir,* 2012, **28**(49), 16788-16797.
11 M. Pouzot, R. Mezzenga, M. Leser, L. Sagalowicz, S. Guillot and O. Glatter, *Langmuir,* 2007, **23**(19), 9618-9628.
12 L. Sagalowicz, S. Guillot, S. Acquistapace, B. Schmitt, M. Maurer, A. Yaghmur, L. de Campo, M. Rouvet, M. Leser and O. Glatter, *Langmuir,* 2013, **29**(26), 8222-8232.
13 I. Martiel, L. Sagalowicz and R. Mezzenga, *Adv. Colloid Interface Sci.,* 2014**, 209**, 127-143.
14 I. Martiel, L. Sagalowicz and R. Mezzenga, *Langmuir,* 2014**, 29**, 15805-15812.
15 B. Angelov, A. Angelova, M. Ollivon, C. Bourgaux and A. Campitelli, *J. Am. Chem. Soc.,* 2003, **125**(24), 7188-7189.
16 B. Angelov, A. Angelova, B. Papahadjopoulos-Sternberg, S. Lesieur, J. F. Sadoc, M. Ollivon and P. Couvreur, *J. Am. Chem. Soc.,* 2006, **128**(17), 5813-5817.
17 B. Angelov, A. Angelova, V. M. Garamus, G. Lebas, S. Lesieur, M. Ollivon, S. S. Funari, R. Willumeit and P. Couvreur, *J. Am. Chem. Soc.,* 2007, **129**(44), 13474-13479.
18 R. Mezzenga, M. Grigorov, Z. Zhang, C. Servais, L. Sagalowicz, A. I. Romoscanu, V. Khanna and C. Meyer, *Langmuir,* 2005, **21**(14), 6165-6169.
19 J. O. Radler, I. Koltover, T. Salditt and C. R. Safinya, *Science,* 1997, **275**(5301), 810-814.
20 A. Bilalov, J. Elsing, E. Haas, C. Schmidt and U. Olsson, *J. Colloid. Interface Sci.,* 2013, **394,** 360-367.
21 S. Phan, W. K. Fong, N. Kirby, T. Hanley and B. J. Boyd, *Int. J. Pharm.,* 2011, **421**(1), 176-182.
22 R. Mezzenga, P. Schurtenberger, A. Burbidge and M. Michel, *Nat. Mater.,* 2005, **4**(10), 729-740.
23 S. Vauthey, C. Milo, P. Frossard, N. Garti, M. E. Leser and H. J. Watzke, *J. Agric. Food Chem.,* 2000, **48**(10), 4808-4816.
24 N. J. Krog, *Food Emulsions,*1997.
25 J. S. Patton and M. C. Carey, *Science,* 1979, **204**(4389), 145-148.
26 S. Mann and G. A. Ozin, *Nature,* 1996, **382**(6589), 313-318.
27 D. D. Archibald and S. Mann, *Nature,* 1993, **364**(6436), 430-433.
28 M. Caffrey, D. Li and A. Dukkipati, *Biochemistry,* 2012, **51**(32), 6266-6288.
29 K. Larsson, *Curr. Opin. Colloid. Interface Sci.,* 2000, **5**(1), 64-69.
30 C. R. Safinya, *Curr. Opin. Struct. Biol.,* 2001, **11**(4), 440-448.
31 C. Fong, T. Le and C. J. Drummond, *Chem. Soc. Rev.,* 2012, **41**(3), 1297-1322.
32 A. Angelova, B. Angelov, V. M. Garamus, P. Couvreur and S. Lesieur, *J. Phys. Chem. Lett.,* 2012, **3**(3), 445-457.
33 J. Barauskas, M. Johnsson and F. Tiberg, *Nano Lett.,* 2005, 5(8), 1615-1619.
34 D. Danino, E. Kesselman, G. Saper, H. I. Petrache and D. Harries, *Biophys. J.,* 2009, **96**(7), L43-L45.
35 S. Deshpande, E. Venugopal, S. Ramagiri, J. R. Bellare, G. Kumaraswamy, N. Singh, *ACS Appl. Mater. Interfaces,* 2014, **6**(19), 17126-17133.
36 J. N. Israelachvili, *Intermolecular and surface forces. 3rd edition*, Academic Press, New York, 2011.
37 H. E. Warriner, S. H. J. Idziak, N. L. Slack, P. Davidson and C. R. Safinya, *Science,* 1996, **271**(5251), 969-973.
38 C. Ligoure, G. Bouglet and G. Porte, *Phys. Rev. Lett.,* 1993, **71**(21), 3600.
39 E. Z. Radlinska, T. Gulik-Krzywicki, F. Lafuma, D. Langevin, W. Urbach and C. E. Williams, *J. de Physique II,* 1997, 7(10), 1393-1416.
40 A. Pal, P. Bharath, S. G. Dastidar and V. A. Raghunathan, *Soft Matter,* 2012, **8**(4), 927-930.
41 Y. Yang, R. Prudhomme, K. M. McGrath, P. Richetti and C. M. Marques, *Phys. Rev. Lett.,* 1998, **80**(12), 2729-2732.
42 C. Nicot, M. Waks, R. Ober, T. Gulik-Krzywicki and W. Urbach, *Phys. Rev. Lett.,* 1996, **77**(16), 3485-3488.
43 L. Ramos and C. Ligoure, *Langmuir,* 2008, **24**(10), 5221-5224.
44 T. Auth and G. Gompper, *Phys. Rev. E,* 2003, 68(5), 051801.
45 A. R. Menjoge, R. M. Kannan and D. A. Tomalia, *Drug Discov. Today,* 2010, **15**(5), 171-185.
46 K. P. Sharma, C. K. Choudhury, S. Srivastava, H. Davis, P. R. Rajamohanan, S. Roy and G. Kumaraswamy, *J. Phys. Chem. B,* 2011, **115**, 9059-9069.

Soft Matter Accepted Manuscript

47 S. W. I. Siu, K. Pluhackova and R. A. Böckmann, *J. Chem. Theory Comput.,* 2012, **8**(4), 1459.
48 M. L. P. Price, D. Ostrovsky and W. L. Jorgensen, *J. Comput. Chem.,* 2001, **22**(13), 1340.
49 W. L. Jorgensen, D. S. Maxwell and J. Tirado-Rives, *J. Am. Chem. Soc.,* 1996, **118**(45), 11225.
50 Y. Sun and P. A. Kollman, *J. Comput. Chem.,* 1995, **16**(9), 1164.
51 J. Briggs, H. Chung and M. Caffrey, *J. de Physique II*, 1996, **6**(5), 723.
52 J. Bornà, T. Nylander and A. Khan, *Langmuir* 2000, **16**(26), 10044.
53 R. C. Rizzo and W. L. Jorgensen, *J. Am. Chem. Soc.,* 1999, **121**(20), 4827.
54 P. Carbone and F. Müller-Plathe, *Soft Matter,* 2009, **5**(13), 2638.
55 S. Nawaz and P. Carbone, *J. Phys. Chem. B,* 2011, **115**(42), 12019.
56 A. Topp, B. J. Bauer, T. J. Prosa, R. Scherrenberg and E. J. Amis, *Macromolecules* 1999, **32**(26), 8923.
57 S. Goudeau, M. Charlot and F. Müller-Plathe, *J. Phys. Chem. B,* 2004, **108**(48), 18779.
58 S. Chakraborty, C. K. Choudhury and S. Roy, *Macromolecules* 2013, **46**(9), 3631.
59 S. Pahari, C. K. Choudhury, P. R. Pandey, M. More, A. Venkatnathan and S. Roy, *J. Phys. Chem. B,* 2012, **116**(24), 7357.
60 H. A. Karimi-Varzaneh, P. Carbone and F. Müller-Plathe, *Macromolecules* 2008, **41**(19), 7211.
61 B. Hess, H. Bekker, H. J. C. Berendsen and J. G. E. M. Fraaije, *J. Comput. Chem.,* 1997, **18**(12), 1463.
62 B. Hess, C. Kutzner, D. Van Der Spoel and E. Lindahl, *J. Chem. Theory Comput.,* 2008, **4**(3), 435.
63 T. Darden, D. York and L. Pedersen, *J. Chem. Phys.,* 1993 **98**(12), 10089.
64 D. Frenkel and B. Smit, Understanding molecular simulation: From algorithms to applications, Academic Press, New York, 2001
65 H. J. C. Berendsen, J. P. M. Postma, W. F. Van Gunsteren, A. Di Nola and J. R. Haak, *J. Chem. Phys.,* 1984, **81**(8), 3684.2222
66 G. Bussi, D. Donadio and M. Parrinello, *J. Chem. Phys.,* 2007, **126**(1), 014101.
67 J. W. Lee, J. H. Kim, H. J. Kim, S. C. Han, J. H Kim, W. S. Shin and S. H. Jin, *Bioconjugate Chem.,* 2007, **18**(2), 579-584.
68 H. Wang, J. Zhuang and S. Thayumanavan, *ACS Macro Lett.,* 2013, **2**(10), 948-951.
69 D. Rousseau, *Food Res. Int.,* 2000, **33**(1), 3-14.
70 A. Ganem-Quintanar, D. Quintanar-Guerrero and P. Buri, *Drug Dev. Ind. Pharma,* 2000, **26**(8), 809-820.
71 C. V. Kulkarni, et al., *Phys. Chem. Chem. Phys.,* 2011, **13**(8), 3004-3021.
72 H. Qiu and M. Caffrey, *Biomaterials,* 2000, **21**(3), 223-234.
73 T. Landh, *J. Phys. Chem.,*1994, **98**(34), 8453-8467.
74 H. H. Lee, W. Y. Jeong, J. K. Kim, K. J. Ihn, J. A. Kornfield, Z. G. Wang and S. Qi, *Macromolecules,* 2002, **35**(3), 785-794.
75 M. Caffrey, *Biochemistry,*1987, **26**(20), 6349-6363.
76 F. Caboi, G. S. Amico, P. Pitzalis, M. Monduzzi, T. Nylander and K. Larsson, *Chem. Phys. Lipids,* 2001, **109**(1), 47-62.
77 S. J. Marrink and D. P. Tieleman, *Biophysical J.,* 2002, 83(5), 2386-2392.
78 A. Salonen, F. Muller and O. Glatter, *Langmuir,* 2008, **24**(10), 5306-5314
79 M. Dulle and O. Glatter, *Langmuir,* 2011, **28**(2), 1136-1141
80 A. Salonen, F. Muller and O. Glatter, *Langmuir,* 2010, **26**(11), 7981-7987

Soft Matter Accepted Manuscript

This journal is © The Royal Society of Chemistry 20xx